

# Finite-temperature critical behaviors in 2D long-range quantum Heisenberg model

Jiarui Zhao,<sup>1</sup> Menghan Song,<sup>1</sup> Yang Qi,<sup>2,3,4</sup> Junchen Rong,<sup>5,\*</sup> and Zi Yang Meng<sup>1,†</sup>

<sup>1</sup>*Department of Physics and HKU-UCAS Joint Institute of Theoretical and Computational Physics, The University of Hong Kong, Pokfulam Road, Hong Kong SAR, China*

<sup>2</sup>*State Key Laboratory of Surface Physics, Fudan University, Shanghai 200438, China*

<sup>3</sup>*Center for Field Theory and Particle Physics, Department of Physics, Fudan University, Shanghai 200433, China*

<sup>4</sup>*Collaborative Innovation Center of Advanced Microstructures, Nanjing 210093, China*

<sup>5</sup>*Institut des Hautes Études Scientifiques, 91440 Bures-sur-Yvette, France*

(Dated: June 5, 2023)

The well-known Mermin-Wagner theorem prohibits the existence of finite-temperature spontaneous continuous symmetry breaking phase in systems with short-range interactions at spatial dimension  $D \leq 2$  [1–3]. For long-range interaction with monotonic power-law form ( $1/r^\alpha$ ), the theorem further forbids a ferro- or antiferromagnetic order at finite temperature when  $\alpha \geq 2D$  [4]. However, the situation for  $\alpha \in (2, 4)$  at  $D = 2$  is beyond the predicting power of the theorem and the situation is still unclear. Here we address this question by large-scale quantum Monte Carlo simulations, accompanied with field theoretical analysis. We find the spontaneous breaking of the  $SU(2)$  symmetry for  $\alpha \in (2, 4)$  in ferromagnetic Heisenberg model with  $1/r^\alpha$  interaction at  $D = 2$ , and obtain the accurate critical exponents by finite-size analysis for  $\alpha < 3$  where the system is above the upper critical dimension with Gaussian fixed point and for  $3 \leq \alpha < 4$  where the system is below the upper critical dimension with non-Gaussian fixed point. Our results reveal the novel critical behaviors in 2D long-range Heisenberg models and will intrigue further experimental studies of quantum materials with long-range interaction beyond the realm of the Mermin-Wagner theorem.

**Introduction.**— In recent years, the importance of the studies on long-range (LR) lattice models have been gradually noticed, due to the fact that they exhibit intrinsically different novel properties from their short-ranged counterparts. For example, LR Heisenberg models at spatial dimension  $D = 2$  acquires anomalous magnon dispersion different from the linear and quadratic spin-waves in the short-range antiferromagnetic and ferromagnetic models [5, 6]. In addition, the violation of Mermin-Wagner theorem and unconventional critical properties in long-range systems also attracted much attention in investigations of both quantum spin models and interacting fermion models [7–30].

These new phenomena also have immediate experimental relevance. Due to the fast development in the Rydberg atom arrays [31–35], the magic angle twisted bilayer Graphene and other 2D quantum moiré materials [36–87] and the programmable quantum simulators [88–92] such as quantum gases coupled to optical cavities [93]. Long-range interactions in the forms of van der Waals, dipole-dipole and Coulomb have given rise to a plethora of correlated topological and quantum phases of matter beyond the semi-classical or mean-field type descriptions, and new theoretical paradigm that could cope with these fast emergent experimental facts are critically called for.

One particularly interesting direction is the critical properties of finite temperature phase transition with continuous symmetry breaking, outside the realm of the established Mermin-Wagner theorem. It was known that, for  $D = 2$  Heisenberg model with ferromagnetic long-range interaction  $1/r^\alpha$ , a finite temperature ferromagnetic phase will not exist when  $\alpha \geq 4$  [4], and for  $\alpha \leq 2$  the system is gapped due to the generalized Higgs mech-

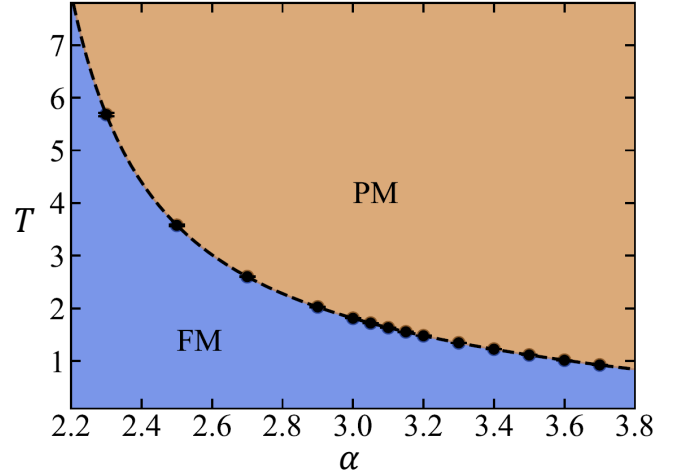


FIG. 1. **Phase diagram of the 2D LR ferromagnetic Heisenberg model.** As the temperature is reduced, the system undergoes a continuous phase transition from paramagnetic phase to ferromagnetic phase in entire region of  $\alpha \in (2, 4)$ . The black dots are the critical points determined from QMC simulations, as exemplified in Figs. 2, 3 and in SM [94].

anism [5, 6]. However, the situation in  $\alpha \in (2, 4)$  is not well understood. Although there are classical field theory predictions and renormalization group analysis on this issue [7, 8, 11], which state there is a Gaussian fixed point for  $2 < \alpha < 3$  and a non-Gaussian fixed-point for  $3 \leq \alpha < 4$ , a thorough numerical treatment on the 2D quantum Heisenberg model has not been performed to date. Such unbiased numerical analysis of this model is

crucial not only because the field-theory scenario needs to be unbiasedly examined on the realistic lattice models, but also due to the fact that the Heisenberg model is one of the most central toy models in condensed matter and statistic physics and a complete clarification of the critical properties of this model will serve as the cornerstone of further studies on LR quantum many body systems.

Here we address this question by large-scale quantum Monte Carlo simulations. We find clear evidence of the breakdown of the Mermin-Wagner theorem with finite temperature phase transitions in  $\alpha \in (2, 4)$ . By performing the state-of-the-art finite size scaling analysis, we obtain the accurate critical exponents of the phase transition as a function of  $\alpha$ , and demonstrate these results nicely satisfy the field-theory predictions both for  $\alpha < 3$  where the system is above the upper critical dimension with Gaussian fixed point and for  $3 \leq \alpha < 4$  where the system is below the upper critical dimension with non-Gaussian fixed point. Our results explicitly show the novel critical behaviors for  $\alpha \in (2, 4)$  in long-range Heisenberg model at  $D = 2$  and will intrigue further theoretical and experimental physics and even mathematics studies of systems with long-range interactions beyond the realm of the Mermin-Wagner theorem [7–12, 95].

*Model and Method.*— The Hamiltonian of the LR ferromagnetic Heisenberg model is

$$\mathcal{H} = - \sum_{i < j} J_{ij} \mathbf{S}_i \mathbf{S}_j, \quad (1)$$

where  $J_{ij} = \frac{1}{r_{ij}^\alpha}$  denotes the long-range coupling and  $r_{ij}$  is the nearest distance between site  $i$  and site  $j$  under the periodic boundary condition. In order to alleviate the strong finite-size effects in systems with long-range interactions, we replace  $J_{ij}$  with the Ewald-corrected coupling  $\tilde{J}_{ij}$  [25, 26] which takes the form of

$$\tilde{J}_{ij} = \sum_{m, n = -\infty}^{\infty} \frac{1}{|\mathbf{i} - \mathbf{j} + mL_x \mathbf{e}_x + nL_y \mathbf{e}_y|^\alpha}. \quad (2)$$

This modified coupling parameter  $\tilde{J}_{ij}$  counts all the possible distances between two sites under the periodic boundary condition. For 2D there is no closed form for Eq. (2), so we truncate the summation at  $|m|_{\max}, |n|_{\max} = 1000$  for  $\alpha < 3$  which is large enough to have the well-converged finite-size scaling behavior, as shown in Fig. 2.

When  $\alpha \geq 2D$  the system reduces to the short-range case where there is no spontaneously continuous symmetry breaking phase at finite temperature. When  $\alpha \leq D$ , the Hamiltonian is no longer extensive and there is no well-defined thermodynamic limit. Between  $\alpha \in (2, 4)$  we carry out the QMC simulations [6, 96, 97] up to the linear system size of  $L = 256$ , as shown in Fig. 2, to determine the precise phase boundary as well as the critical exponents  $\nu$ ,  $\beta$  and  $\eta$ . The results are shown in Figs. 1 and 3 and will be discussed in the results section. The

QMC implementation is explained in the Supplementary Materials (SM) [94].

Note that when  $\alpha \leq D$ , the Hamiltonian defined in Eq. (1) can actually be Kac-normalized [98, 99] to be extensive with the addition of a factor  $\frac{N-1}{\sum_{i < j} J_{ij}}$  to the Hamiltonian. Although this is not the focus of our paper, we examine the Kac-normalized Hamiltonian at  $\alpha = 1.8$  and the results are shown in Fig. 4 and in SM [94].

*Finite size scaling analysis.*— To identify the phase transition and obtain the critical exponents, we compute the square magnetization  $\langle m^2 \rangle$ , the correlation function  $G(r)$ , and the Binder ratio  $U(T, L) = \frac{\langle m^4 \rangle}{\langle m^2 \rangle^2}$  in the QMC simulation. The crossing point of  $U(T, L)$  with  $U(T, 2L)$  is denoted as  $T^*(L)$  and it is expected to converge to the thermodynamic limit critical temperature  $T_c$  following the scaling relation:

$$T^*(L) = aL^{-b} + T_c. \quad (3)$$

Given the values of  $T^*(L)$  with sufficiently small errors and large enough system sizes  $L$ , the critical point  $T_c$  can be precisely located. To obtain the critical exponents  $\nu$ ,  $\beta$  and  $\eta$ , when  $D \leq D_{\text{uc}}$ , the standard finite-size scaling behavior (FSS) [100, 101] allows us to perform a data collapse near the critical points with the relation

$$m^2 \sim L^{-2\beta/\nu} \cdot f \left[ L^{1/\nu} (T - T_c) \right], \quad T \sim T_c. \quad (4)$$

The anomalous dimension can also be obtained by fitting to the correlation function at the critical point  $T_c$

$$G(r) = \langle S_{\mathbf{r}}^z S_{\mathbf{r}+\mathbf{r}}^z \rangle \sim r^{-D+2-\eta}. \quad (5)$$

However, when  $D > D_{\text{uc}}$ , which is our case when  $\alpha < 3$ , the system enters the mean-field region where the hyperscaling relation breaks down, famously due to the effect of dangerously irrelevant operator [102]. The scaling of the correlation length in this region shall follow the relation  $\xi_L \sim L^{\frac{D_{\text{uc}}}{D}}$  instead of  $\xi_L \sim L$  [14, 25, 26, 103, 104], and this leads to the modification of hyperscaling relation with

$$\nu' d = 2 - \alpha_H \quad (6)$$

where  $\nu' = \frac{D_{\text{uc}}}{D} \nu$  and  $\alpha_H$  is the critical exponent associated with the specific heat. For our system Eq. (1), the upper critical dimension is  $D_{\text{uc}} = 2(\alpha - D)$ , which we will explain later in the field theory analysis section. Accordingly, Eq. (4) also needs to be modified and the correct relation for data collapse in mean field region is [14, 25, 26, 103, 104]

$$m^2 \sim L^{-2\beta/\nu'} \cdot f \left[ L^{1/\nu'} (T - T_c) \right], \quad T \sim T_c. \quad (7)$$

The scaling of correlation function for  $\alpha < 3$  is also modified with

$$G(r) = \langle S_{\mathbf{r}}^z S_{\mathbf{r}+\mathbf{r}}^z \rangle \sim r^{-D+2-\eta_Q}, \quad (8)$$

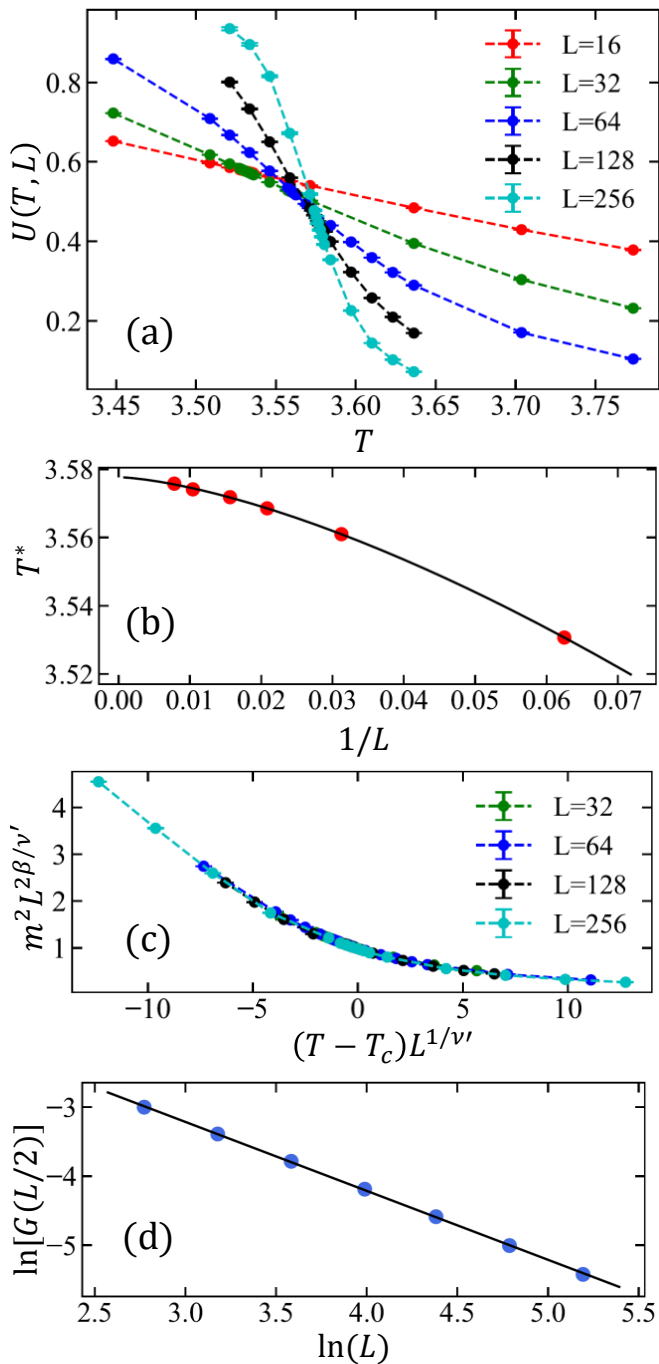


FIG. 2. **The determination of the critical point and exponents at  $\alpha = 2.5$ .** (a) Binder ratio  $U(T, L)$  versus temperature  $T$  for different system sizes. (b) Crossing points of Binder ratios  $T^*(L)$  versus  $1/L$ . The solid line represents a fitting of the data points with Eq. (3). The fitted curve is  $T^*(L) = -2.935L^{-1.491} + 3.5776$ . (c) Data collapse of the order parameter  $\langle m^2 \rangle$  near the critical point  $T_c$ . Notice here we replace the correlation length exponent  $\nu$  with  $\nu'$  as in Eq. (7). (d)  $\ln[G(L/2)]$  versus  $\ln(L)$  for different system sizes  $L = 16, 24, 36, 54, 80, 120, 180$ . The data is fitted with a straight line as in Eq. (8) and the fitted result is  $\ln[G(L/2)] = -0.999(1) \ln(L)$ . The errors of  $\ln[G(L/2)]$  are smaller than the symbol sizes.

where

$$\eta_Q = \frac{D}{D_{uc}} \eta - \frac{2D}{D_{uc}} + 2. \quad (9)$$

By fitting to Eq. (8), the modified anomalous dimension  $\eta_Q$  as well as  $\eta$  can be obtained.

To unify the conventions, we define

$$\eta_Q = \begin{cases} \frac{D}{D_{uc}} \eta - \frac{2D}{D_{uc}} + 2, & \text{if } D > D_{uc}, \\ \eta, & \text{if } D \leq D_{uc}. \end{cases} \quad \nu' = \begin{cases} \frac{D_{uc}}{D} \nu, & \text{if } D > D_{uc}, \\ \nu, & \text{if } D \leq D_{uc}. \end{cases} \quad (10)$$

Then  $\nu'$ ,  $\beta$  and  $\eta_Q$  will be obtained with the same scaling functions for both  $\alpha < 3$  and  $3 \leq \alpha < 4$ .

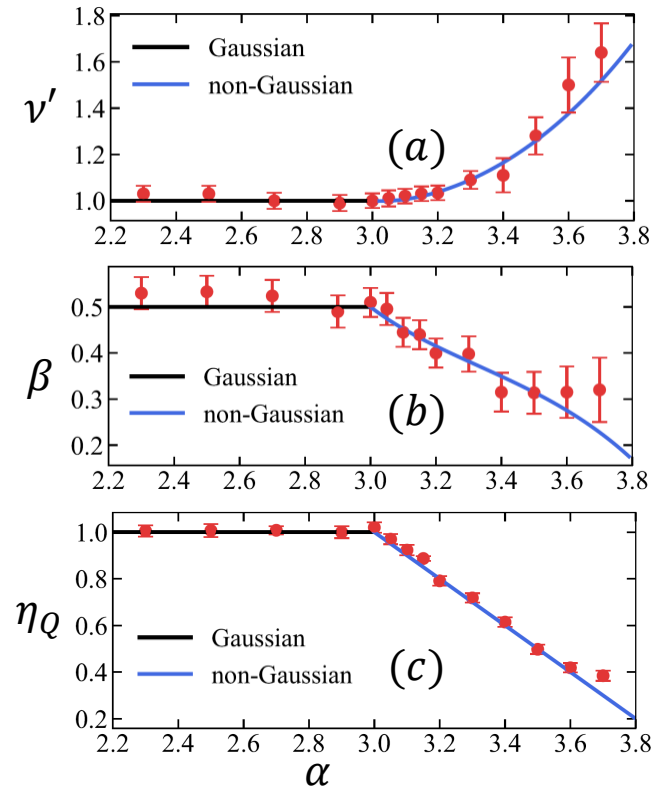


FIG. 3. **Critical exponents  $\nu'$ ,  $\beta$  and  $\eta_Q$  in the region of  $\alpha \in [2.3, 3.7]$  obtained from data collapse and from fitting to the correlation function  $G(r)$ .** The black and blue solid lines in (a), (b) and (c) are the predictions of long-range Gaussian theory ( $\alpha < 3$ ) and two-loop perturbative RG predictions ( $3 \leq \alpha < 4$ ) for Gaussian and interacting (non-Gaussian) fixed points. [7, 8, 10].

*Field theory analysis.*— We review here the field theory description of the model at the thermodynamic limit dating back to Ref. [7]. The action can be written as

$$S = \int d^D x d^D x' \frac{\phi(x)\phi(x')}{|x-x'|^{d+\sigma}} + \lambda \int d^D x \phi(x)^4, \quad (11)$$

to match the lattice model, we need  $\alpha = d + \sigma$ . Under the scaling symmetry

$$x \rightarrow sx, \phi \rightarrow s^{-\Delta_\phi} \phi, \quad (12)$$

the kinetic term remains unchanged when  $\Delta_\phi = \frac{D-\sigma}{2}$ . The coupling constant of  $\phi^4$  interaction, on the other hand, scale as

$$\lambda \rightarrow s^{2\alpha-3D}\lambda. \quad (13)$$

When  $\alpha < \frac{3D}{2}$ , the coupling constant decays at larger length scale, which means the  $\lambda\phi^4$  term is an irrelevant operator. The Gaussian fixed point at  $\lambda = 0$  is a stable fixed point. This was established mathematically in Ref. [10]. When  $\alpha > \frac{3D}{2}$ , the  $\lambda\phi^4$  term becomes relevant, which triggers a renormalization group towards a new non-Gaussian fixed point [7]. One can perform standard renormalization technique to calculate the scaling dimension of various operators, by evaluating Feynman diagrams with non-conventional propagators. Such a calculation was first performed in [7]. Since the kinetic term in Eq. (11) is no-local, which can not receive corrections from any local counter terms, the scaling dimension of  $\phi$  will not be renormalized (This can be easily seen by analysing the Callan-Symanzik equation for the two point function  $\langle\phi(x)\phi(y)\rangle$ , see for example, Ref. [105]). Equivalently, we have  $\eta = 2\Delta_\phi - D + 2$ . Our numerical result clearly confirms such a theoretical prediction. For a fixed  $\sigma$  in Eq. (11), we can define the upper critical dimension as the space-time dimension at which the  $\phi^4$  term is marginal. The  $\Delta_{\phi^4} = 4\Delta_\phi = D_{uc}$  gives us

$$D_{uc} = 2\sigma = 2(\alpha - D). \quad (14)$$

We now focus on the  $D = 2$  case. When  $\alpha < 3$ , the critical behaviour is controlled by the  $\lambda = 0$  Gaussian fixed point. The critical behaviour is similar to the usual Ising model at  $D > 4$ , due to the effect of dangerously irrelevant operators [102], the critical exponents are given by

$$\nu = \frac{1}{\alpha - 2}, \quad \beta = \frac{1}{2}, \quad \eta = 4 - \alpha. \quad (15)$$

For example, the  $\beta = 1/2$  exponent can be seen from the following argument. Deform the action (11) by a mass term  $\int dx^D t\phi(x)^2$  with negative  $t$  and minimise the potential, we get  $\langle\phi\rangle \propto (-t/\lambda)^\beta$ , with  $\beta = 1/2$ . The other exponents can be calculated by similar mean field theory analysis. The critical exponent  $\eta$  controls the two point function  $\langle\phi(x)\phi(y)\rangle$  only at the strict thermodynamic limit. At finite size, the power law behaviour will be modified to (8), which follows from analysing the effect of dangerously irrelevant operators carefully [104].

When  $\alpha > 3$ , on the other hand, the second term in Eq. (11) becomes relevant, and renormalization group flows towards a new non-Gaussian fixed point [7]. The critical exponent  $\eta$  will remain at its mean field theory value [7] as in Eq. (15). The other exponents, on the other hand receives correction at  $\mathcal{O}((\alpha - 3)^2)$ . The two-

loop perturbation results for  $\gamma$  is

$$\frac{1}{\gamma} = 1 - \left(\frac{n+2}{n+8}\right) \frac{\epsilon}{\sigma} - \frac{(n+2)(7n+20)}{(n+8)^3} Q(\sigma) \left(\frac{\epsilon}{\sigma}\right)^2 + \mathcal{O}(\epsilon^3) \quad (16)$$

with  $Q(\sigma) = \sigma [\psi(1) - 2\psi(\frac{1}{2}\sigma) + \psi(\sigma)]$  where  $\psi(z)$  is the logarithmic derivative of the gamma function. The other critical exponents can be obtained by scaling relations between them.

When  $\alpha > 4$ , the long range model becomes equivalent to short range models, due to the Mermin-Wagner theorem [1-3], the system will be gapped at finite temperature.

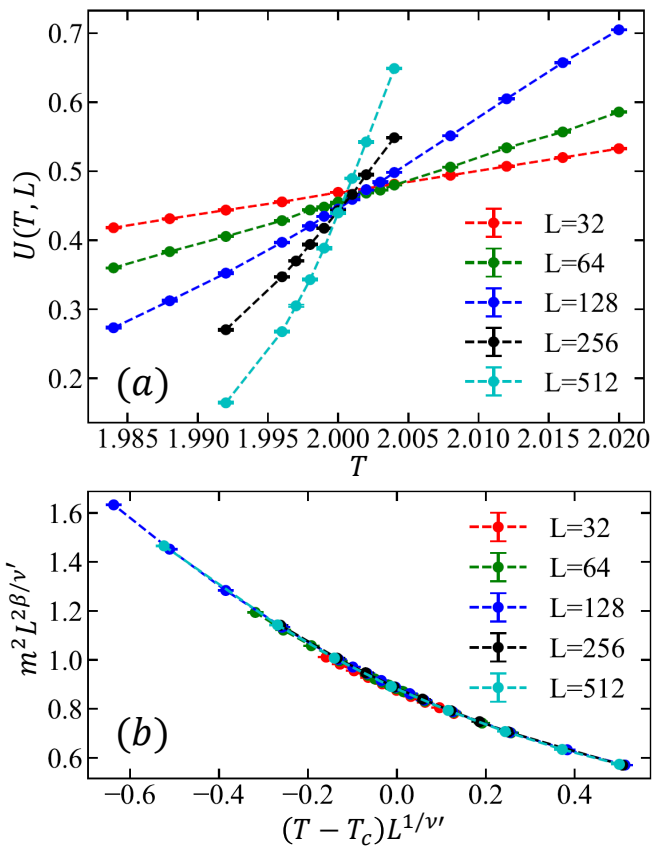


FIG. 4. **The determination of the critical point and exponents at  $\alpha = 1.8$ .** (a) Binder ratio  $U(T, L)$  versus temperature  $T$  for different system sizes. (b) Data collapse of the order parameter  $\langle m^2 \rangle$  near the critical point  $T_c$ . The obtained results are  $\nu' = 1.00(5)$  and  $\beta = 0.505(8)$ .

**Results.**— Fig. 2 shows our results at  $\alpha = 2.5$ . We first use the crossing points of the Binder ratios to locate the critical temperature  $T_c$ . The crossing points of  $U(T, L)$  with  $U(T, 2L)$  are denoted as  $T^*(L)$ , and through fitting to Eq. (3) the precise value of  $T_c$  can be obtained. We then use the value of  $T_c$  to perform data collapse according to Eq. (4) and Eq. (7) separately for  $3 \leq \alpha < 4$  and  $\alpha < 3$ , to obtain the critical exponents  $\nu'$  and  $\beta$ . To obtain the anomalous dimension  $\eta_Q$ , we measure the cor-



relation function  $G(L/2)$  at the obtained critical temperature  $T_c$  and obtain the anomalous dimension separately by fitting to Eq. (5) for  $3 \leq \alpha < 4$  and Eq. (8) for  $\alpha < 3$ .

According to the conventions defined in Eq. (10) and field theory results of the mean-field critical exponents in Eq. (15), we can extract the expression for the three critical exponents in the Gaussian region which are  $\nu' = 1$ ,  $\beta = \frac{1}{2}$  and  $\eta_Q = 1$ . Outside the Gaussian region, we have  $\eta = 4 - \alpha$  and  $\gamma$  defined in Eq. (16) and the value of  $\beta$  and  $\nu$  can be obtained via solving the scaling relations between the critical exponents with  $\nu = \frac{\gamma}{2-\eta}$  and  $\beta = \frac{\gamma\eta}{2(2-\eta)}$ .

The fitting results are shown in Fig. 3. We find that within the region we simulated, our QMC-obtained critical exponents  $\nu'(\alpha)$ ,  $\beta(\alpha)$ , and  $\eta_Q(\alpha)$  match nicely with the prediction of both long-range Gaussian theory (for  $\alpha < 3$ ) and the two-loop perturbative RG (for  $3 \leq \alpha < 4$ ). Notably, the anomalous dimension  $\eta$  receive no corrections at any  $\alpha \in (2, 4)$  [7] and our results confirm this argument with  $\eta$  matches with  $\eta = 4 - \alpha$  well in the whole region.

Note that we also examine the case where  $\alpha = 1.8$  with a Kac-normalized Hamiltonian as shown in Fig. 4. The obtained values of  $\beta$  and  $\nu'$  indicate at  $\alpha < D$  the system is still governed by the mean-field fixed point. More details for the case  $\alpha < 2$  will be discussed in the SM [94].

*Discussions.*— Our results clearly point out the LR quantum many-body system exhibit unconventional critical properties beyond the realm of the Mermin-Wagner theorem [7–12, 95], which are worthwhile to pursue in experimental systems where the LR interactions in the forms of van der Waals, dipole-dipole and Coulomb play the dominate role. Such systems include, but not limited to, Rydberg arrays, twisted bilayer Graphene and 2D quantum Moiré material and quantum simulators.

*Acknowledgment.*— We thank Subir Sachdev, Fabien Alet, Fakher Assaad, Kai Sun, Michael Scherer and Lukas Janssen for valuable discussions on the related topic. JRZ thanks Mr. Tianyu Wu and Ms. Zhenzhi Qin for valuable discussions. JRZ, MHS and ZYM acknowledge the support from the Research Grants Council (RGC) of Hong Kong SAR of China (Project Nos. 17301420, 17301721, AoE/P-701/20, 17309822, HKU C7037-22G), the ANR/RGC Joint Research Scheme sponsored by RGC of Hong Kong and French National Research Agency (Project No. A\_HKU703/22), the K. C. Wong Education Foundation (Grant No. GJTD-2020-01) and the Seed Fund “Quantum-Inspired explainable-AI” at the HKU-TCL Joint Research Centre for Artificial Intelligence. The authors also acknowledge the Tianhe-II platform at the National Supercomputer Center in Guangzhou, the HPC2021 system under the Information Technology Services and the Blackbody HPC system at the Department of Physics, University of Hong Kong for

their technical support and generous allocation of CPU time.

---

\* junchenrong@gmail.com

† zymeng@hku.hk

- [1] P. C. Hohenberg, Phys. Rev. **158**, 383 (1967).
- [2] N. D. Mermin and H. Wagner, Phys. Rev. Lett. **17**, 1133 (1966).
- [3] B. I. Halperin, Journal of Statistical Physics **175**, 521 (2019).
- [4] P. Bruno, Phys. Rev. Lett. **87**, 137203 (2001).
- [5] O. K. Diessel, S. Diehl, N. Defenu, A. Rosch, and A. Chiocchetta, arXiv e-prints, arXiv:2208.10487 (2022), arXiv:2208.10487 [cond-mat.quant-gas].
- [6] M. Song, J. Zhao, C. Zhou, and Z. Y. Meng, arXiv e-prints, arXiv:2301.00829 (2023), arXiv:2301.00829 [cond-mat.str-el].
- [7] M. E. Fisher, S.-k. Ma, and B. G. Nickel, Phys. Rev. Lett. **29**, 917 (1972).
- [8] J. Sak, Phys. Rev. B **8**, 281 (1973).
- [9] M. Aizenman and R. Fernández, Letters in Mathematical Physics **16**, 39 (1988).
- [10] M. Lohmann, G. Slade, and B. C. Wallace, Journal of Statistical Physics **169**, 1132 (2017).
- [11] J. Sak, Phys. Rev. B **15**, 4344 (1977).
- [12] G. Slade, Communications in Mathematical Physics **358**, 343 (2017).
- [13] N. Defenu, T. Donner, T. Macrì, G. Pagano, S. Ruffo, and A. Trombettoni, arXiv e-prints, arXiv:2109.01063 (2021), arXiv:2109.01063 [cond-mat.str-el].
- [14] E. G. Lazo, M. Heyl, M. Dalmonte, and A. Angelone, SciPost Phys. **11**, 076 (2021).
- [15] S. Birnkammer, A. Bohrdt, F. Grusdt, and M. Knap, Phys. Rev. B **105**, L241103 (2022).
- [16] D. Peter, S. Müller, S. Wessel, and H. P. Büchler, Phys. Rev. Lett. **109**, 025303 (2012).
- [17] J. Ren, Z. Wang, W. Chen, and W.-L. You, Phys. Rev. E **105**, 034128 (2022).
- [18] C. Hou and C. M. Varma, Phys. Rev. B **94**, 201101 (2016).
- [19] L. Zhu, C. Hou, and C. M. Varma, Phys. Rev. B **94**, 235156 (2016).
- [20] P. Adelhardt and K. P. Schmidt, arXiv e-prints, arXiv:2209.01182 (2022), arXiv:2209.01182 [cond-mat.quant-ph].
- [21] C. J. Hamer, Z. Weihong, and P. Arndt, Phys. Rev. B **46**, 6276 (1992).
- [22] Z. Li, S. Choudhury, and W. V. Liu, Phys. Rev. A **104**, 013303 (2021).
- [23] S. Jenkins, L. Rózsa, U. Atxitia, R. F. Evans, K. S. Novoselov, and E. J. Santos, Nature Communications **13**, 6917 (2022).
- [24] M. F. Maghrebi, Z.-X. Gong, and A. V. Gorshkov, Phys. Rev. Lett. **119**, 023001 (2017).
- [25] J. A. Koziol, A. Langheld, S. C. Kapfer, and K. P. Schmidt, Phys. Rev. B **103**, 245135 (2021).
- [26] E. J. Flores-Sola, B. Berche, R. Kenna, and M. Weigel, The European Physical Journal B **88** (2015), 10.1140/epjb/e2014-50683-1.
- [27] Y. Da Liao, X. Y. Xu, Z. Y. Meng, and Y. Qi, arXiv

- e-prints , arXiv:2210.04272 (2022), arXiv:2210.04272 [cond-mat.str-el].
- [28] Z. Wang, F. Assaad, and M. Ulybyshev, arXiv e-prints , arXiv:2211.02960 (2022), arXiv:2211.02960 [cond-mat.str-el].
- [29] M. Weber, D. J. Luitz, and F. F. Assaad, Phys. Rev. Lett. **129**, 056402 (2022).
- [30] P. Werner, M. Troyer, and S. Sachdev, Journal of the Physical Society of Japan **74**, 67 (2005).
- [31] R. Samajdar, W. W. Ho, H. Pichler, M. D. Lukin, and S. Sachdev, Proceedings of the National Academy of Sciences **118**, e2015785118 (2021).
- [32] Z. Yan, R. Samajdar, Y.-C. Wang, S. Sachdev, and Z. Y. Meng, Nat. Commun. **13**, 5799 (2022).
- [33] G. Semeghini, H. Levine, A. Keesling, S. Ebadi, T. T. Wang, D. Bluvstein, R. Verresen, H. Pichler, M. Kalinowski, R. Samajdar, A. Omran, S. Sachdev, A. Vishwanath, M. Greiner, V. Vuletić, and M. D. Lukin, Science **374**, 1242 (2021).
- [34] K. J. Satzinger, Y. J. Liu, A. Smith, C. Knapp, M. Newman, C. Jones, Z. Chen, C. Quintana, X. Mi, A. Dunsworth, C. Gidney, I. Aleiner, F. Arute, K. Arya, J. Atalaya, R. Babbush, J. C. Bardin, R. Barends, J. Basso, A. Bengtsson, A. Bilmes, M. Broughton, B. B. Buckley, D. A. Buell, B. Burkett, N. Bushnell, B. Chiaro, R. Collins, W. Courtney, S. Demura, A. R. Derk, D. Eppens, C. Erickson, L. Faoro, E. Farhi, A. G. Fowler, B. Foxen, M. Giustina, A. Greene, J. A. Gross, M. P. Harrigan, S. D. Harrington, J. Hilton, S. Hong, T. Huang, W. J. Huggins, L. B. Ioffe, S. V. Isakov, E. Jeffrey, Z. Jiang, D. Kafri, K. Kechedzhi, T. Khattar, S. Kim, P. V. Klimov, A. N. Korotkov, F. Kostritsa, D. Landhuis, P. Laptev, A. Locharla, E. Lucero, O. Martin, J. R. McClean, M. McEwen, K. C. Miao, M. Mohseni, S. Montazeri, W. Mruczkiewicz, J. Mutus, O. Naaman, M. Neeley, C. Neill, M. Y. Niu, T. E. O'Brien, A. Opremcak, B. Pató, A. Petukhov, N. C. Rubin, D. Sank, V. Shvarts, D. Strain, M. Szalay, B. Villalonga, T. C. White, Z. Yao, P. Yeh, J. Yoo, A. Zalcman, H. Neven, S. Boixo, A. Megrant, Y. Chen, J. Kelly, V. Smelyanskiy, A. Kitaev, M. Knap, F. Pollmann, and P. Roushan, Science **374**, 1237 (2021).
- [35] Z. Yan, Y.-C. Wang, R. Samajdar, S. Sachdev, and Z. Y. Meng, Phys. Rev. Lett. **130**, 206501 (2023).
- [36] G. Trambly de Laissardière, D. Mayou, and L. Magaud, Nano Lett. **10**, 804 (2010).
- [37] R. Bistritzer and A. H. MacDonald, Proceedings of the National Academy of Sciences **108**, 12233 (2011).
- [38] J. M. B. Lopes dos Santos, N. M. R. Peres, and A. H. Castro Neto, Phys. Rev. B **86**, 155449 (2012).
- [39] G. Trambly de Laissardière, D. Mayou, and L. Magaud, Phys. Rev. B **86**, 125413 (2012).
- [40] A. Rozhkov, A. Sboychakov, A. Rakhmanov, and F. Nori, Physics Reports **648**, 1 (2016), electronic properties of graphene-based bilayer systems.
- [41] Y. Cao, V. Fatemi, S. Fang, K. Watanabe, T. Taniguchi, E. Kaxiras, and P. Jarillo-Herrero, Nature **556**, 43 (2018).
- [42] Y. Cao, V. Fatemi, A. Demir, S. Fang, S. L. Tomarken, J. Y. Luo, J. D. Sanchez-Yamagishi, K. Watanabe, T. Taniguchi, E. Kaxiras, *et al.*, Nature **556**, 80 (2018).
- [43] Y. Xie, B. Lian, B. Jäck, X. Liu, C.-L. Chiu, K. Watanabe, T. Taniguchi, B. A. Bernevig, and A. Yazdani, Nature **572**, 101 (2019).
- [44] X. Lu, P. Stepanov, W. Yang, M. Xie, M. A. Aamir, I. Das, C. Urgell, K. Watanabe, T. Taniguchi, G. Zhang, *et al.*, Nature **574**, 653 (2019).
- [45] A. Kerelsky, L. J. McGilly, D. M. Kennes, L. Xian, M. Yankowitz, S. Chen, K. Watanabe, T. Taniguchi, J. Hone, C. Dean, *et al.*, Nature **572**, 95 (2019).
- [46] Y. Da Liao, Z. Y. Meng, and X. Y. Xu, Phys. Rev. Lett. **123**, 157601 (2019).
- [47] M. Yankowitz, S. Chen, H. Polshyn, Y. Zhang, K. Watanabe, T. Taniguchi, D. Graf, A. F. Young, and C. R. Dean, Science **363**, 1059 (2019).
- [48] S. L. Tomarken, Y. Cao, A. Demir, K. Watanabe, T. Taniguchi, P. Jarillo-Herrero, and R. C. Ashoori, Phys. Rev. Lett. **123**, 046601 (2019).
- [49] Y. Cao, D. Chowdhury, D. Rodan-Legrain, O. Rubies-Bigorda, K. Watanabe, T. Taniguchi, T. Senthil, and P. Jarillo-Herrero, Phys. Rev. Lett. **124**, 076801 (2020).
- [50] C. Shen, Y. Chu, Q. Wu, N. Li, S. Wang, Y. Zhao, J. Tang, J. Liu, J. Tian, K. Watanabe, T. Taniguchi, R. Yang, Z. Y. Meng, D. Shi, O. V. Yazyev, and G. Zhang, Nature Physics (2020).
- [51] K. P. Nuckolls, M. Oh, D. Wong, B. Lian, K. Watanabe, T. Taniguchi, B. A. Bernevig, and A. Yazdani, Nature **588**, 610 (2020).
- [52] T. Soejima, D. E. Parker, N. Bultinck, J. Hauschild, and M. P. Zaletel, Phys. Rev. B **102**, 205111 (2020).
- [53] S. Chatterjee, M. Ippoliti, and M. P. Zaletel, Phys. Rev. B **106**, 035421 (2022).
- [54] E. Khalaf, N. Bultinck, A. Vishwanath, and M. P. Zaletel, arXiv preprint arXiv:2009.14827 (2020).
- [55] M. Xie and A. H. MacDonald, Phys. Rev. Lett. **124**, 097601 (2020).
- [56] E. Khalaf, S. Chatterjee, N. Bultinck, M. P. Zaletel, and A. Vishwanath, Science Advances **7** (2021).
- [57] A. T. Pierce, Y. Xie, J. M. Park, E. Khalaf, S. H. Lee, Y. Cao, D. E. Parker, P. R. Forrester, S. Chen, K. Watanabe, *et al.*, Nature Physics **17**, 1210 (2021).
- [58] Y.-D. Liao, X.-Y. Xu, Z.-Y. Meng, and J. Kang, Chinese Physics B **30**, 017305 (2021).
- [59] A. Rozen, J. M. Park, U. Zondiner, Y. Cao, D. Rodan-Legrain, T. Taniguchi, K. Watanabe, Y. Oreg, A. Stern, E. Berg, *et al.*, Nature **592**, 214 (2021).
- [60] U. Zondiner, A. Rozen, D. Rodan-Legrain, Y. Cao, R. Queiroz, T. Taniguchi, K. Watanabe, Y. Oreg, F. von Oppen, A. Stern, *et al.*, Nature **582**, 203 (2020).
- [61] Y. Saito, F. Yang, J. Ge, X. Liu, T. Taniguchi, K. Watanabe, J. Li, E. Berg, and A. F. Young, Nature **592**, 220 (2021).
- [62] J. M. Park, Y. Cao, K. Watanabe, T. Taniguchi, and P. Jarillo-Herrero, Nature **592**, 43 (2021).
- [63] Y. H. Kwan, Y. Hu, S. H. Simon, and S. A. Parameswaran, Phys. Rev. Lett. **126**, 137601 (2021).
- [64] Y. Da Liao, J. Kang, C. N. Breiø, X. Y. Xu, H.-Q. Wu, B. M. Andersen, R. M. Fernandes, and Z. Y. Meng, Phys. Rev. X **11**, 011014 (2021).
- [65] J. Kang, B. A. Bernevig, and O. Vafek, Phys. Rev. Lett. **127**, 266402 (2021).
- [66] J. Liu and X. Dai, Phys. Rev. B **103**, 035427 (2021).
- [67] F. Schindler, O. Vafek, and B. A. Bernevig, Phys. Rev. B **105**, 155135 (2022).
- [68] E. Brillaux, D. Carpentier, A. A. Fedorenko, and L. Savary, Phys. Rev. Research **4**, 033168 (2022).
- [69] Z.-D. Song and B. A. Bernevig, Phys. Rev. Lett. **129**, 047601 (2022).

- [70] J.-X. Lin, Y.-H. Zhang, E. Morissette, Z. Wang, S. Liu, D. Rhodes, K. Watanabe, T. Taniguchi, J. Hone, and J. Li, *Science* **375**, 437 (2022).
- [71] S. Bhowmik, B. Ghawri, N. Leconte, S. Appalakondiah, M. Pandey, P. S. Mahapatra, D. Lee, K. Watanabe, T. Taniguchi, J. Jung, *et al.*, *Nature Physics*, 1 (2022).
- [72] T. Huang, X. Tu, C. Shen, B. Zheng, J. Wang, H. Wang, K. Khaliji, S. H. Park, Z. Liu, T. Yang, *et al.*, *Nature* **605**, 63 (2022).
- [73] S. Zhang, X. Lu, and J. Liu, *Phys. Rev. Lett.* **128**, 247402 (2022).
- [74] J. Herzog-Arbeitman, A. Chew, D. K. Efetov, and B. A. Bernevig, *Phys. Rev. Lett.* **129**, 076401 (2022).
- [75] E. Y. Andrei and A. H. MacDonald, *Nature Materials* **19**, 1265 (2020).
- [76] P. Stepanov, M. Xie, T. Taniguchi, K. Watanabe, X. Lu, A. H. MacDonald, B. A. Bernevig, and D. K. Efetov, *Phys. Rev. Lett.* **127**, 197701 (2021).
- [77] G. Pan, X. Zhang, H. Lu, H. Li, B.-B. Chen, K. Sun, and Z. Y. Meng, *Phys. Rev. Lett.* **130**, 016401 (2023).
- [78] X. Zhang, G. Pan, Y. Zhang, J. Kang, and Z. Y. Meng, *Chinese Physics Letters* **38**, 077305 (2021).
- [79] J. S. Hofmann, E. Khalaf, A. Vishwanath, E. Berg, and J. Y. Lee, *Phys. Rev. X* **12**, 011061 (2022).
- [80] G. Pan, X. Zhang, H. Li, K. Sun, and Z. Y. Meng, *Phys. Rev. B* **105**, L121110 (2022).
- [81] X. Zhang, G. Pan, X. Y. Xu, and Z. Y. Meng, *Phys. Rev. B* **106**, 035121 (2022).
- [82] X. Zhang, K. Sun, H. Li, G. Pan, and Z. Y. Meng, *Phys. Rev. B* **106**, 184517 (2022).
- [83] X. Zhang, G. Pan, B.-B. Chen, H. Li, K. Sun, and Z. Y. Meng, *arXiv e-prints*, arXiv:2210.11733 (2022), arXiv:2210.11733 [cond-mat.str-el].
- [84] B.-B. Chen, Y. D. Liao, Z. Chen, O. Vafek, J. Kang, W. Li, and Z. Y. Meng, *Nature Communications* **12**, 5480 (2021).
- [85] X. Lin, B.-B. Chen, W. Li, Z. Y. Meng, and T. Shi, *Phys. Rev. Lett.* **128**, 157201 (2022).
- [86] M. Huang, Z. Wu, X. Zhang, X. Feng, Z. Zhou, S. Wang, Y. Chen, C. Cheng, K. Sun, Z. Y. Meng, and N. Wang, *arXiv e-prints*, arXiv:2212.12666 (2022), arXiv:2212.12666 [cond-mat.mes-hall].
- [87] C. Huang, X. Zhang, G. Pan, H. Li, K. Sun, X. Dai, and Z. Y. Meng, *arXiv e-prints*, arXiv:2304.14064 (2023), arXiv:2304.14064 [cond-mat.str-el].
- [88] R. Verresen, M. D. Lukin, and A. Vishwanath, *Phys. Rev. X* **11**, 031005 (2021).
- [89] R. Samajdar, D. G. Joshi, Y. Teng, and S. Sachdev, *arXiv e-prints*, arXiv:2204.00632 (2022), arXiv:2204.00632 [cond-mat.quant-gas].
- [90] Z. Yan, X. Ran, Y.-C. Wang, R. Samajdar, J. Rong, S. Sachdev, Y. Qi, and Z. Y. Meng, *arXiv e-prints*, arXiv:2205.04472 (2022), arXiv:2205.04472 [cond-mat.str-el].
- [91] X. Ran, Z. Yan, Y.-C. Wang, J. Rong, Y. Qi, and Z. Y. Meng, *arXiv e-prints*, arXiv:2209.10728 (2022), arXiv:2209.10728 [cond-mat.str-el].
- [92] Y.-C. Wang, M. Cheng, W. Witczak-Krempa, and Z. Y. Meng, *Nature Communications* **12**, 5347 (2021).
- [93] H. Ritsch, P. Domokos, F. Brennecke, and T. Esslinger, *Rev. Mod. Phys.* **85**, 553 (2013).
- [94] The linear spin wave analysis for the LR ferromagnetic and staggered AFM Heisenberg models and detailed data on the fitting of the excitation gaps from the dynamical correlation functions in QMC are shown in this Supplementary Materials.
- [95] A. Abdesselam, *Communications in mathematical physics* **276**, 727 (2007).
- [96] A. W. Sandvik and J. Kurkijärvi, *Phys. Rev. B* **43**, 5950 (1991).
- [97] A. W. Sandvik, *Phys. Rev. B* **59**, R14157 (1999).
- [98] E. G. Lazo, M. Heyl, M. Dalmonte, and A. Angelone, *SciPost Phys.* **11**, 076 (2021).
- [99] N. Defenu, *Proceedings of the National Academy of Sciences* **118**, e2101785118 (2021).
- [100] M. E. Fisher, S.-k. Ma, and B. G. Nickel, *Phys. Rev. Lett.* **29**, 917 (1972).
- [101] E. Brézin, *J. Phys. France* **43**, 15 (1982).
- [102] J. Cardy, *Scaling and renormalization in statistical physics*, Vol. 5 (Cambridge university press, 1996).
- [103] Kenna and Berche, *Condensed Matter Physics* **16**, 23601 (2013).
- [104] R. Kenna and B. Berche, *Europhysics Letters* **105**, 26005 (2014).
- [105] C. Behan, L. Rastelli, S. Rychkov, and B. Zan, *Journal of Physics A: Mathematical and Theoretical* **50**, 354002 (2017).
- [106] A. J. Walker, *ACM Transactions on Mathematical Software (TOMS)* **3**, 253 (1977).
- [107] K. Fukui and S. Todo, *Journal of Computational Physics* **228**, 2629 (2009).

## SUPPLEMENTARY MATERIALS

### SSE QMC update scheme

The Hamiltonian defined in Eq. (1) can be decomposed as diagonal and off-diagonal operators,

$$\begin{aligned} H_{0,0} &= I \\ H_{1,a(ij)} &= J_{ij} \left( \frac{1}{4} + S_i^z S_j^z \right) \\ H_{2,a(ij)} &= \frac{J_{ij}}{2} (S_i^+ S_j^- + S_i^- S_j^+), \end{aligned} \quad (17)$$

where  $H - \frac{\sum_{i<j} J_{ij}}{4} = -\sum_{a(i<j)} H_{1,a(ij)} + H_{2,a(ij)}$  and  $a(ij)$  is the bond index. Take the eigenstates of  $\sigma^z$  as basis, the non-zero matrix elements in Eq. (17) are

$$\begin{aligned} \langle \uparrow\uparrow | H_{1,a} | \uparrow\uparrow \rangle &= \langle \downarrow\downarrow | H_{1,a} | \downarrow\downarrow \rangle = \frac{J_{ij}}{2} \\ \langle \uparrow\downarrow | H_{2,a} | \downarrow\uparrow \rangle &= \langle \downarrow\uparrow | H_{2,a} | \uparrow\downarrow \rangle = \frac{J_{ij}}{2}. \end{aligned} \quad (18)$$

In the SSE QMC simulation, the loop update scheme is maintained the same with the ferromagnetic Heisenberg model with nearest-neighbor couplings. However, to efficiently carry out the diagonal update scheme, we choose the candidate bonds for inserting diagonal operators with an importance sampling procedure with  $P_{\text{choose}} \propto J_{ij}$ . The diagonal update scheme is thus

1. If a diagonal operator ( $H_{1,a}$ ) is visited, remove it with probability

$$P_{\text{remove}} = \min \left( \frac{2(M-n+1)}{\beta \sum_{i<j} J_{ij}}, 1 \right) \quad (19)$$

2. If an identity operator ( $H_{0,a}$ ) is visited, insert a diagonal operator according to:
  - First choose a candidate bond  $a$  to make the insertion with probability

$$P_{\text{choose}} = \frac{J_{ij}}{\sum_{i<j} J_{ij}} \quad (20)$$

- Then accept the insertion of a diagonal operator at this position with probability

$$P_{\text{accept}} = \min \left( \frac{\beta \sum_{i<j} J_{ij}}{2(M-n)}, 1 \right) \quad (21)$$

To generate a set of random bond index according to the probability defined in Eq. (20), we use the naive Walker's method [106] with complexity of  $O(N^2)$ . Despite there is optimization of this method which reduces the complexity to  $O(N)$  [107], we find for the system size we simulate the original method is sufficient and easy to implement. The above procedure ensures that diagonal operators with higher matrix elements have higher probability to be inserted and compared with randomly choosing candidate bonds this strategy certainly has better efficiency.

### Kac normalization and phase diagram at $\alpha < 2$

With a long-range Hamiltonian defined as

$$H = - \sum_{i<j} J_{ij} \mathbf{S}_i \cdot \mathbf{S}_j. \quad (22)$$

The ground state is a fully ferromagnetic state with all spins aligned in the same direction. We have shown in the main text that the system undergoes a continuous phase transition at  $\alpha \in (2, 4)$ . However, when  $\alpha \leq 2$  the system



is no longer extensive and it is still unclear whether such a system still hold a phase transition point. To make the system extensive, a Kac normalization factor can be added to the Hamiltonian and the normalized Hamiltonian is

$$H = -\frac{N-1}{\sum_{i<j} J_{ij}} \sum_{i<j} J_{ij} \mathbf{S}_i \mathbf{S}_j. \quad (23)$$

In this case, the energy density is  $\langle \uparrow \dots \uparrow | H/N | \uparrow \dots \uparrow \rangle = -(N-1)/N$  which will be a constant for any value of  $\alpha$ . For the Hamiltonian defined in Eq. (23), we perform the QMC simulations and find that there is a continuous phase transition for  $\alpha = 1.8$  and the critical exponents also satisfies the prediction of mean-field theory, as shown in Fig. 4. In addition, we also examine this system at other values of  $\alpha$  and we find that the phase transition point  $T_c$  remains the same for all the  $\alpha \leq 2$  we consider, as indicated in Fig. 5. There is an intuitive understanding for this finding: the Kac normalization [98, 99] makes the energy scale to be the same for all  $\alpha \leq 2$  which somehow suppresses the effect of different decaying exponent  $\alpha$  and the phase transition temperature  $T_c$  is thus scaled to be the same for all  $\alpha$ . This point should be further examined by more robust analysis.

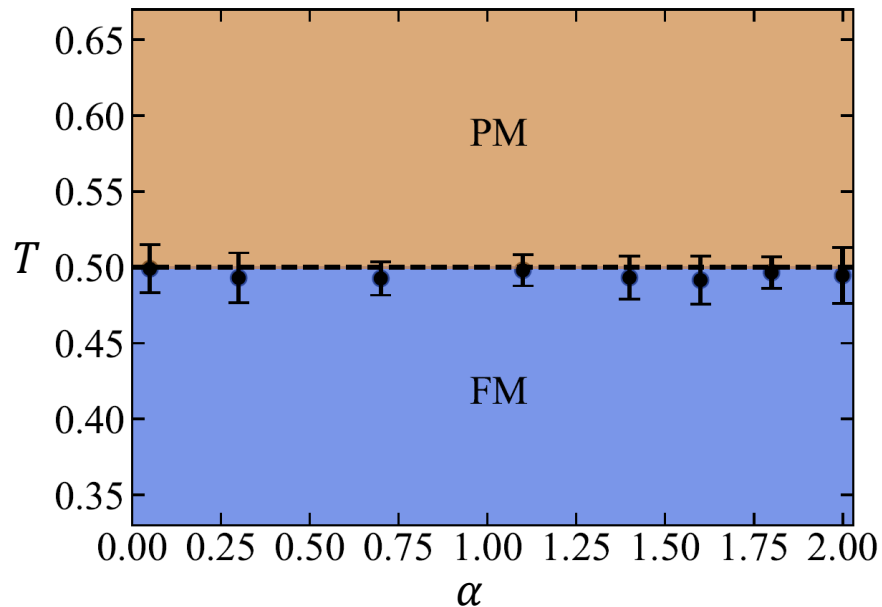


FIG. 5. **Phase diagram of the 2D LR ferromagnetic Heisenberg model with Kac-normalized Hamiltonian.** The system also undergoes a continuous phase transition from FM to PM as temperature is increased. The black dots are the critical points determined from QMC simulations.